RSC Advances

RSC Advances

www.rsc.org/advances

ROYAL SOCIETY OF CHEMISTRY

www.rsc.org/advances

RSC Advances

ARTICLE

Concave Gold Nanoparticles Based Highly Sensitive Electrochemical IgG Immunobiosensor by Antibody-Antigen Interactions

Youju Huang, *[a,b,†] Palanisamy Kannan,[c,†] Lei Zhang,[a] Tao Chen*[a] and Dong-Hwan Kim*[b]

In this work, we report a novel electrochemical sensor for the label-free, real time and highly sensitive detection of antibody-antigen interactions based on concave gold nanocuboids (CAuNCs). In contrast to low-index facets AuNPs such as gold nanorods (AuNRs), the CAuNCs provide higher surface atoms with enhanced chemical activities, which can efficiently catalyse the oxidation reaction of amino groups on antibody (Anti-bovine IgG produced in rabbit). This leads to an obvious redox current response was observed in cyclic voltammetry (CV) measurement. Upon the introduction of IgG antigen, notable decrease of anodic peak current was observed, which is attributed to the formation of an antigen–antibody complex between the IgG antigen and antibody on CAuNCs. The unique electro-catalytic property of CAuNCs allows to easily detecting the rabbit IgG antigen in a wide range of concentration (from 10 to 200 ng mL^{-1}) with a limit of detection (LOD) to 5 ng mL^{-1} (signal to noise ratio 3 (S/N=3)) by using CV method.

1. Introduction

Accurate and sensitive detection of proteins is of great significance in both biomedical research and clinical diagnosis.[1-3] Numerous immunoassay methods such as fluorescence,[4] chemiluminescence,[5] surface plasmon,[6,7] and mass spectrometric immunoassays[8] have been developed for the detection of different proteins.[9-11] Though, these methods often suffer from considerable time consumption, high cost and tediously professional operation, which make them imperfect candidate for practical applications and demand a more convenient detection method with a comparable or even higher sensitivity.[12-14] In this sense, the electrochemical label-free immunoassay is ideal for detection of proteins and has recently aroused extensive interest due to its rapid recognition, simple instrumentation and easy operation.[15,16]

Antibodies are large Y-shaped protein molecules produced by the immune system, which are typically used to identify and neutralize foreign objects such as bacteria and viruses.[17-20] Their excellent reorganization and binding properties provide numerous opportunities in various applications such as biological research, biotechnology, and medicine.[20,21] The characterization of antibody-antigen interactions has therefore long been a hot topic of research. Generally, there are two typical detection approaches (electrochemical and optical techniques) to this kind of immunological sensing.[20,22] Compared with optical techniques such as fluorescence fluctuation spectroscopy (FFS)[23] and colloidal Au–

enhanced localized surface plasmon resonance (LSPR),[24] electrochemical method offers some advantages such as simple design and fabrication , small dimensions, low power requirement and low cost.[25]

Among the various electrochemical techniques, electrochemical impedance spectroscopy is a common method to detect the antibody-antigen interactions.[26,27] In this case, after the introduction of antigen, a thick antibody–antigen complexes layer should be formed on the electrode surface, which leads to the changes of resistance. This allows detecting the antibody-antigen interactions by monitoring the electrochemical impedance response. Although cyclic voltammetry (CV) is the most widely used technique for acquiring qualitative information about electrochemical reactions based on the detection of antibody-antigen interactions.[28,29] This is mainly because the direct electron transfer (DET) between an electrode and immobilized proteins is rarely produced, especially, without redox mediators in system.

Recent development in nanotechnology offers excellent opportunities for the sensible design of functional nanomaterials with unique surface and electronic properties for electrochemical immunoassay.[30,31] The large surface-to-volume ratio of nanomaterials ensures the immobilization of a sufficient amount of recognition elements, while the high electronic conductivity, excellent catalytic activity and biocompatibility provide significantly improved signal transductions.[32-35] As a result, high sensitivity, good selectivity, low detection limit, fast response, and miniaturization of the sensing devices can be achieved.[32,33] Therefore, nanomaterial can facilitate electron transfer or electro-catalyse the oxidation reaction of antibody, is an important and necessary to modify on the electrodes. In this view point, anisotropic gold nanoparticles exhibit high chemical and plasmonic sensitivity as well as multiple plasmon resonance bands[36-39] along with their individual axes, this enables tuning the plasmon resonance from visible to near-IR spectral regions.[40,41] Inspired by such appealing optical and

[a] Division of Polymer and Composite Materials, Ningbo Institute of Material Technology and Engineering, Chinese Academy of Science, 1219 Zhongguan West Road, Ningbo 315201, China.
E-mail: yjhuang@nimte.ac.cn; E-mail: tao.chen@nimte.ac.cn;
[b] School of Chemical and Biomedical Engineering (SCBE), Nanyang Technological University, Singapore. E-mail: dhkim@ntu.edu.sg
[c] Singapore Centre on Environmental Life Science Engineering (SCELSE), Nanyang Technological University, Singapore.
† These authors contribute equally to this work.

chemical properties of anisotropic AuNPs, we have synthesized concave Au rectangular nanocuboids (CAuNCs) by seeded growth method.[42] It is very important to mention that, the CAuNCs are not common nanostructures, and generally possess high-index facets {720}, which exhibit much higher chemical activities[40,41,43] and superior electrocatalytic performance, compared with conventional AuNPs enclosed by low-index facets such as {111}, {100}, and {110}.[44-47] Despite a potentially marked influence of these concave AuNPs, there, to the best of our knowledge, is no report on applications of concave AuNPs in electrochemical sensors, probably due to challenges in synthesis, which arises from their high surface energy. In this paper, we report a simple route based on seeded growth to the synthesis of Au concave nanocuboids bounded by high index{720} facets (CAuNCs) were synthesized by a simple route and then used to develop a highly sensitive label-free electrochemical immunobiosensor. Due to the higher electrocatalytic activity of CAuNCs, the as-proposed sensor shows great potential towards the detection of rabbit IgG antigen. The observed result indicates that as-prepared CAuNCs very promising candidates for practical clinical purposes.

2. Experimental Section

2.1. Chemical and Regents. Hydrogen tetrachloroaurate trihydrate ($HAuCl_4 \cdot 3H_2O$) was purchased from Sigma-Aldrich, Singapore. Trisodium citrate, sodium borohydride ($NaBH_4$), cetyltrimethylammonium bromide (CTAB), silver nitrate ($AgNO_3$), and ascorbic acid (AA) were purchased from Merck (Singapore) and were used as received. All other chemicals used in this investigation were of analytical grade and were used without further purification. The 0.2 M phosphate buffer (PB) solution was prepared from Na_2HPO_4 and NaH_2PO_4, and a freshly prepared solution of AA was used in all the experiments. Double-distilled water was used to prepare all the experimental solutions.

2.2. Instrumentation. UV-visible spectra were recorded with a PerkinElmer Lamda 35 spectrophotometer. Scanning electron microscopic measurements were performed with a JEOL JSM6700F field emission scanning electron microscope. Electrochemical measurements were performed in a conventional two-compartment three-electrode cell with a mirror polished 3 mm glassy carbon (GC) as the working electrode, Pt wire as the counter electrode, and a NaCl saturated Ag/AgCl as the reference electrode. The electrochemical measurements were carried out with a CHI model 670D electrochemical workstation (Austin, TX, U.S.A). All the electrochemical experiments were carried out under a nitrogen atmosphere. The immunobiosensor design and detection principle is shown in Figure 1. Herein, the sandwich-type immunobiosensing approach was adopted. Prior to the modification, the glassy carbon electrode was pre-treated with polishing and ultrasonic cleaning. First the 3 μl of CAuNCs were deposited on the glass carbon electrode, and allow for 3 hr for drying under nitrogen atmosphere. After that, the electrode was incubated in an anti-rabbit IgG solution for 12 hr at 4°C. As a result, the anti-IgG was immobilized on the electrode through electrostatic interaction. In order to prevent nonspecific adsorption, the unreacted sites were blocked with 2% BSA in PBS (pH 7.4) for 1 hr at 4°C. Subsequently, the modified electrode was used as a probe to detect rabbit IgG.

2.2. Preparation of AuNR seeds. AuNR seed preparation includes two subsequent experimental steps based on our previous report[42] i.e., the formation of spherical Au seeds (~3 nm in diameter) followed by a growth of AuNR seeds (~61 nm in length and ~18 nm in width). Briefly, the spherical Au seeds was prepared by the addition of a freshly prepared, ice-cold, aqueous $NaBH_4$ solution

(0.01 M, 0.6 mL) into an aqueous mixture composed of $HAuCl_4$ (0.01M, 0.25 mL) and CTAB (0.1 M, 9.75 mL). The resultant solution was mixed by rapid inversion for 2 min and then kept at room temperature for at least 2 h before use. To fabricate AuNR seeds, a growth solution was prepared by mixing an aqueous solution of $HAuCl_4$ (0.01 M, 4 mL), $AgNO_3$ (0.01 M, 0.8 mL), and CTAB (0.1 M, 80 mL) together. Then, a freshly prepared, aqueous ascorbic acid solution (0.1 M, 0.64 mL) was added to the above mixture, followed by the addition of an aqueous HCl solution (1.0 M, 1.6 mL). The resultant solution was mixed by rapid inversion, followed by the addition of the spherical Au seed solution (0.02 mL). The above mixture was subjected to gentle inversion for 10 s and then left undisturbed for at least 6 h, resulting in forming AuNR seeds.
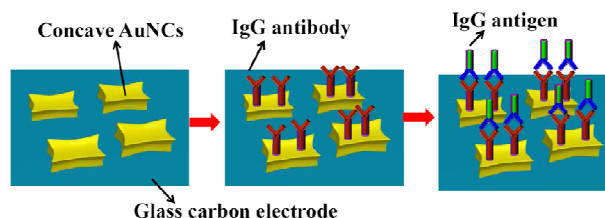
Figure 1. Schematic representation of the immunobiosensor design and the detection principle.

2.3. Preparation of concave Au nanocuboids. The Au nanocuboids was prepared according to our previous report.[42] 7.5 mL of a growth solution containing a mixture of 2.5×10^{-4} M $HAuCl_4$ and 0.01 M CTAB solutions were added to five 20 mL conical flasks. Then, 41 μL of 0.1 M freshly prepared ascorbic acid was added into each flask followed by gentle stirring for 2 min. Finally, 0.2 mL of the AuNR seed solutions at different concentrations (0.2 C_0, 0.5 C_0, C_0, 2 C_0 and 5 C_0, where C_0 represents concentration of AuNR seed stock solution) were added into each flask and the mixtures were kept at 30°C in water bath for at least 6 hours. The concentrated AuNR seed solution (i.e., 5 C_0 and 2 C_0) were prepared by re-dispersing centrifuged precipitation of AuNR seeds into 0.1 M CTAB solution.

3. Results and Discussion.

3.1. Morphological Characterization of CAuNCs. In a typical synthesis, an aqueous solution of ascorbic acid was injected (with a pipette) into a mixture containing $HAuCl_4$ and CTAB solutions under magnetic stirring. Then AuNR seeds were added to the above reaction mixture, and allow at 30°C in water bath for at least 6 hr (*vide supra*). A closer examination indicates that a small portion of the cubes were somewhat elongated along one of the axes to form rectangular bars with aspect ratios (length to width) slightly larger than one (Figure 2a). Since both the cubes and bars were enclosed by {001} facets, they are collectively called "nanocuboids" for easiness. We have discussed that the creation of concave structures is not thermodynamically favourable, particularly for the case of seeded growth,[48] the growth rate of atoms on seeds can be manipulated by kinetic control.[48] As the concentration of AuNR seeds plays an essential role in the control of nanoparticle growth, we have optimized various seed concentrations ranging from $5 \times C_0$ to $0.2 \times C_0$ (C_0 represents concentration of AuNR seed stock solution) to obtain concave nanoparticles, and the resultant products are designated as AuNP-$5C_0$, AuNP-$2C_0$, AuNP-C_0, AuNP-$0.5C_0$, and AuNP-$0.2C_0$ respectively.[42] It has been known that the higher seed concentration of $5 \times C_0$ has been frequently used for AuNP synthesis.[49-51] Such higher seed concentration normally leads to

isotropic overgrowth of Au seeds, resulting in the formation of a rod-like nanostructure with flat surfaces.[42] When the seed concentration is reduced to $2 \times C_0$, grown AuNPs begin to exhibit facets with irregular trapezoidal and triangular structures on the surface.[42] The concave nanocuboids can be obtained in moderate seed concentration between $0.5 \times C_0$ and to $1 \times C_0$ (Figure 2a). The AuNPs synthesized at a concentration of $1 \times C_0$ (AuNPC$_0$) was used as a representative seed for concave nanocuboids throughout the experiment.
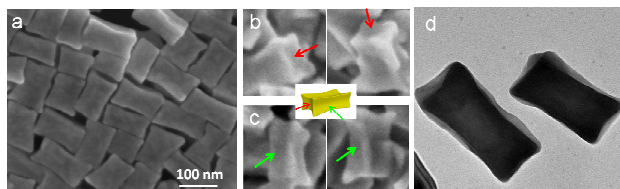
Figure 2. Representative FE-SEM images of Au nanocuboids (a), synthesized at the AuNR seed concentrations of $1 \times C_0$. The close examination of edges of concave structure (b, and c) focused from the single Au nanocuboids. The corresponding HR-TEM image of CAuNCs is shown in image d.

The nanoparticles products were extensively characterized by FE-SEM (Figure 2b and c). As you see the side view or top view, the nanoparticles appear to have a well clear concave morphology. The FE-SEM images show that the faces of the caves each have contrast lines in the shape of a wide "X" (Figure 2b and c). The size of the concave nanocuboids, as determined by edge length, can be adjusted from tens to hundreds of nanometers by varying the volume of seed particles added to the growth solution. Therefore, concave cuboids with edge lengths of 50 ± 5 nm (Figure 2b), and 100 ± 5 nm (Figure 2c) can be synthesized by our optimized protocol. The FE-SEM images of these nanoparticles show that the concave faces of the cuboids are maintained regardless of particle size, although the facets are better defined or more easily assignable for most of the larger particles. To completely characterize the structure of the concave nanocuboids, the facets on its surface are indexed. The high-index facets of an Au nanocuboids can be theoretically obtained by the interfacial angles.[52] The average measured angle is 17±1°, indicating that the facets of the concave cubes are indeed high-index {720} facets, which have a calculated angle of 16.0°. Note that few facets appear to have a slightly larger angle such as 18°-19°, which can be attributed to a different high-index facets such as {510}, {830}, and {310}.[42] From the angles of several concave nanocubes, we could conclude that the surface of a Au concave nanocuboids was mainly enclosed by {720} facets, together with few other high-index facets such as {510}, {830}, and {310}. A similar structure was recently reported by Mirkin and co-workers for concave nanocubes of Au, the surface of which was enclosed by mostly {720} and some {310} planes.[52] Overall, we have obtained the facets of the concave cubes are mostly {720} planes, mixed with few {510}, {830}, and {310} planes. A similar observation has also been made for the electrochemically prepared Pt tetrahexahedral nanoparticles, where, in addition to the most prevalent {730} planes, a few other planes such as {520}, {210}, and {310} planes were also identified.[53] The morphological and structural characterizations were further confirmed by HR-TEM image (Figure 2d), the concave nanocuboids enclosed by 24 high-index {720} facets. The sizes of these concave

nanocubes could be controlled in the range of 50–100 nm by simply using Au nanorods with different edge lengths as the seeds. We found that a low volume of Au nanorods was beneficial to the formation of Au concave nanocuboids by preferential overgrowth at corner and edge sites of a rod seed.

3.2. Electrochemical Characterization of CAuNCs. The deposition of CAuNCs on GC electrode was characterized by cyclic voltammetry (CV) method. The CVs obtained for AuNRs, and CAuNCs modified GC electrodes in 0.1M H_2SO_4 solution were shown in Figure 3. The AuNRs modified GC electrode shows an oxidation peak at 1.26V and a corresponding reduction peak at 0.9V (Figure 3a). The redox peaks are attributed to the oxidation and subsequent reduction of surface gold oxide (AuOx) formation of the AuNRs, as a result of the positive potential polarization of the AuNRs modified GC electrode. On the other hand, CAuNCs modified GC electrode shows an oxidation peak at 1.15V, which is 0.11V less positive potential than AuNRs, and a corresponding distinguished reduction peak at 0.9V (Figure 3b). The amount of Au oxide exposed to the solution was calculated by integrating the charge under the Au oxide reduction peak corrected for the baseline, and it was found to be 33.84μC.[54] We have calculated the particle coverage (θ_p) of CAuNCs GC electrode using Equ. (1). The particle coverage is defined as the ratio between the electrochemically accessible CAuNCs area and the geometric area of the GC electrode in contact with the electrolyte solution.[55] The particle coverage of CAuNCs modified GC electrode was calculated by using the charge involved in the reduction of electrochemically formed Au oxide from the CV recorded, between the potential window from 1.0 to 0.5V in 0.1M H_2SO_4 solution, by assuming the charge density for the reduction peak of the Au oxide is 723μC/cm^2.[55]
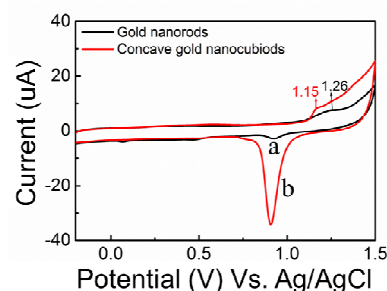
Figure 3. CVs obtained for AuNRs (a), and CAuNCs (b) modified GC electrodes in 0.1M H_2SO_4 solution at a scan rate of 50mVs^{-1}.

$$\theta_p = \frac{\text{Au Oxide Charge (μC) / 723 (μC/cm}^2)}{\text{GC Electrode Geometric Area (cm}^2)} \quad \text{------- (1)}$$

The CAuNCs particle coverage on GC electrode was found to be 19.79%. However, AuNRs deposited electrode showed only 1.45% of particles coverage. Therefore, the CAuNCs showed very higher particle coverage on GC electrode, which is effectively utilized for immobilizing large amount of IgG antibody for detecting IgG protein.

3.3. Electrochemical IgG Immunobiosensor. To study the potential utilization of IgG antibody/CAuNCs modified electrode, the electrocatalytic oxidation and electrochemical determination of IgG antigen were carried out in 0.2 M PB Solution (pH 7.2). The AuNRs/GC electrode does not give any electrochemical response for

IgG antibody, and IgG antigen-antibody immobilization on CAuNCs, shown in Figure 4A, curve a, and b. This is due to the fact that the surface atoms of AuNRs composed of low index facets (111) cannot catalyze this reaction. Moreover, lower coverage of nanorods (1.45%) may not allow large amount antibody and antigens on its surface. On the other hand, CAuNCs electrode showed a broad oxidation peak at ~0.45V, and corresponding reduction peak at 0.01V, respectively (Figure 4B, curve a). The above oxidation is mainly because of functional amino groups present in the IgG antibody involved electrochemical oxidation in PB solution. The observed result is closely matched with the oxidation of gold nanoparticles based polymer film nanocomposite electrode.[56] From the CV, as can see CAuNCs modified electrode have clear response in presence of IgG antibody and antibody-antigen interactions. The CAuNCs possesses high index facets {720}, which can provide higher electrochemically active atoms/sites for this oxidation reaction. However, the electrochemical response disappeared at ~0.45V and 0.01V (Figure 4B, curve b), a new peak was observed at ~0.25V due
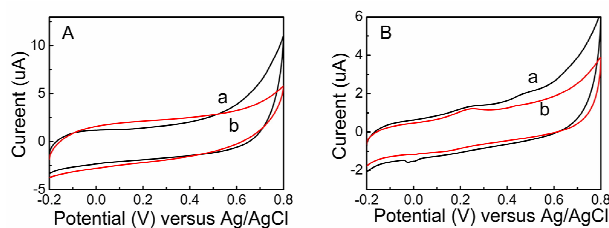
Figure 4. CVs obtained for IgG antibody (a), and IgG antigen-antibody (b) on AuNRs (A), and CAuNCs (B) modified GC electrodes in 0.2 M PB solution at a scan rate of 50mVs^{-1}.

to the interaction, and complex formation between IgG antigen - IgG antibody. Moreover, the catalytic current response decreases due to the high coverage of IgG antigen on IgG antibody/CAuNCs surface, which results the resistive layer on the electrode. In the presence of IgG antigen molecule, the IgG-antibody incorporated CAuNCs electrode showed a broad oxidation peak for IgG antigen (~0.25V; *vide supra*) clearly indicates that IgG antibody-CAuNCs modified electrode effectively detect the IgG antigen due to the specific interaction of the IgG-incorporated CAuNCs with the IgG antigen. The immobilized CAuNCs provides an efficient catalysis platform for the present IgG immunobiosensor. In other words, the deposition of the whole IgG antibodies on the CAuNCs surface relies on electrostatic interactions *(vide supra)*. Simultaneously, the physical adsorption is one of the protein binding processes, although rather uncontrollable. Random orientation of the assembled antibodies and close proximity between adsorptive surface and the antigen-binding site could enable the detection through impeding CV response. Moreover, the CAuNCs greatly increases the active surface area for loading large amount of IgG antibody. Furthermore, no reduction peak is seen IgG antigen during interaction with IgG antibody modified CAuNCs electrode (Figure 4B, curve a). These results reveal that the oxidation process of IgG antigen at the IgG antibody/CAuNCs electrode is faster than the AuNRs electrode and also the IgG antibody-incorporated CAuNCs electrode possess higher electrocatalytic activity towards the IgG oxidation. The electrochemical response of the IgG antibody/CAuNCs electrode has been investigated as a function of IgG antigen concentration (10–200 ng mL^{-1}) using CV technique

(Figure 5A). The current increase on each addition of IgG is attributed to the formation of an antigen–antibody complex between the IgG antigen and the IgG antibody on CAuNCs.
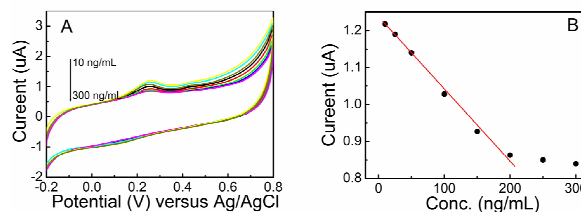
Figure 5. (A) CV recorded for IgG antibody on CAuNCs-modified immunoelectrode as a function of varying concentrations of IgG antigen (a–h); 10, 25, 50, 100, 150, 200, 250 and 300 ng mL^{-1}, respectively, in 0.2 M PB Solution (pH 7.2) at a scan rate of 50 mV s^{-1}. (B) Calibration plot obtained for current response vs. function of conc. of IgG antigen at scan rate of 50 mV s^{-1}.

The Figure 5B shows the calibration curve obtained as a function of IgG antigen concentration. A linear relationship between the magnitude of current and IgG concentration can be fitted to the experimental points from 10 to 200 ng mL^{-1} with a correlation coefficient of 0.9913. The value of association constant (K_a) was calculated to be 5.32×10^{11} l mol^{-1} using a Lineweaver–Burke like plot,[57] indicating high affinity of IgG antibody towards the IgG antigen attributed to prevalent electrostatic interactions. The increased activity of IgG antibody due to favourable electrostatic interaction with CAuNCs results in high value of K_a. The detection limit of IgG Antibody/CAuNCs electrode towards IgG antigen was calculated from CV method, and it was 5 ng mL^{-1} (S/N=3).

Conclusions

We described a novel electrochemical sensor for the label-free, real time and highly sensitive detection of antibody-antigen interactions based on CAuNCs. The CAuNCs provide higher surface atoms with enhanced chemical activities, which can efficiently catalyse the oxidation reaction of amino groups on antibody (Anti-bovine IgG produced in rabbit). This provides an obvious redox current response was observed in CV response and the introduction of IgG antigen, notable decrease of anodic peak current was observed, which reduces the protein mobility so less amine can participate in the electrochemical oxidation reaction after antibody-antigen interactions. The electro-catalytic property of CAuNCs showed an excellent sensing platform towards the rabbit IgG antigen in a wide range of concentration (from 10 to 200 ng mL^{-1}) with a limit of detection (LOD) is 5 ng mL^{-1} (S/N=3) by using CV method.

Acknowledgements

Notes and references

(1)Hucknall, A.; Rangarajan, S.; Chilkoti, A. In Pursuit of Zero: Polymer Brushes that Resist the Adsorption of Proteins. *Adv. Mater.* **2009**, *21*, 2441-2446.
(2)Khatayevich, D.; Page, T.; Gresswell, C.; Hayamizu, Y.; Grady, W.; Sarikaya, M. Selective Detection of Target Proteins by Peptide-Enabled Graphene Biosensor. *Small* **2014**, *10*, 1505-1513.

Journal Name

ARTICLE

(3)Wang, N.; Gao, C.; Han, Y.; Huang, X.; Xu, Y.; Cao, X. Detection of human immunoglobulin G by label-free electrochemical immunoassay modified with ultralong CuS nanowires. *J. Mater. Chem. B* **2015**, *3*, 3254-3259.

(4)Yu, Q.; Wang, X.; Duan, Y. Capillary-Based Three-Dimensional Immunosensor Assembly for High-Performance Detection of Carcinoembryonic Antigen Using Laser-Induced Fluorescence Spectrometry. *Anal. Chem.* **2014**, *86*, 1518-1524.

(5)Ma, F.; Yang, Y.; Zhang, C.-y. Ultrasensitive Detection of Transcription Factors Using Transcription-Mediated Isothermally Exponential Amplification-Induced Chemiluminescence. *Anal. Chem.* **2014**, *86*, 6006-6011.

(6)Lane, J. S.; Richens, J. L.; Vere, K.-A.; O'Shea, P. Rational Targeting of Subclasses of Intermolecular Interactions: Elimination of Nonspecific Binding for Analyte Sensing. *Langmuir* **2014**, *30*, 9457-9465.

(7)Zhang, Y.; Islam, N.; Carbonell, R. G.; Rojas, O. J. Specific Binding of Immunoglobulin G with Bioactive Short Peptides Supported on Antifouling Copolymer Layers for Detection in Quartz Crystal Microgravimetry and Surface Plasmon Resonance. *Anal. Chem.* **2013**, *85*, 1106-1113.

(8)Meyer, K.; Ueland, P. M. Targeted Quantification of C-Reactive Protein and Cystatin C and Its Variants by Immuno-MALDI-MS. *Anal. Chem.* **2014**, *86*, 5807-5814.

(9)Maehashi, K.; Katsura, T.; Kerman, K.; Takamura, Y.; Matsumoto, K.; Tamiya, E. Label-Free Protein Biosensor Based on Aptamer-Modified Carbon Nanotube Field-Effect Transistors. *Anal. Chem.* **2007**, *79*, 782-787.

(10)Lee, J. S.; Joung, H.-A.; Kim, M.-G.; Park, C. B. Graphene-Based Chemiluminescence Resonance Energy Transfer for Homogeneous Immunoassay. *ACS Nano* **2012**, *6*, 2978-2983.

(11)Li, T.; Jo, E.-J.; Kim, M.-G. A label-free fluorescence immunoassay system for the sensitive detection of the mycotoxin, ochratoxin A. *Chem. Commun.* **2012**, *48*, 2304-2306.

(12)Yu, X.; Munge, B.; Patel, V.; Jensen, G.; Bhirde, A.; Gong, J. D.; Kim, S. N.; Gillespie, J.; Gutkind, J. S.; Papadimitrakopoulos, F.; Rusling, J. F. Carbon Nanotube Amplification Strategies for Highly Sensitive Immunodetection of Cancer Biomarkers. *J. Am. Chem. Soc.* **2006**, *128*, 11199-11205.

(13)Wang, G.; Huang, H.; Zhang, G.; Zhang, X.; Fang, B.; Wang, L. Dual Amplification Strategy for the Fabrication of Highly Sensitive Interleukin-6 Amperometric Immunosensor Based on Poly-Dopamine. *Langmuir* **2011**, *27*, 1224-1231.

(14)Campàs, M.; Marty, J.-L. Highly sensitive amperometric immunosensors for microcystin detection in algae. *Biosens. Bioelectron.* **2007**, *22*, 1034-1040.

(15)Yang, L.; Zhao, H.; Fan, S.; Deng, S.; Lv, Q.; Lin, J.; Li, C.-P. Label-free electrochemical immunosensor based on gold–silicon carbide nanocomposites for sensitive detection of human chorionic gonadotrophin. *Biosens. Bioelectron.* **2014**, *57*, 199-206.

(16)Zhou, J.; Xu, M.; Tang, D.; Gao, Z.; Tang, J.; Chen, G. Nanogold-based bio-bar codes for label-free immunosensing of proteins coupling with an in situ DNA-based hybridization chain reaction. *Chem. Commun.* **2012**, *48*, 12207-12209.

(17)Litman, G. W.; Rast, J. P.; Shamblott, M. J.; Haire, R. N.; Hulst, M.; Roess, W.; Litman, R. T.; Hinds-Frey, K. R.; Zilch, A.; Amemiya, C. T. Phylogenetic diversification of immunoglobulin genes and the antibody repertoire. *Mol. Bio. Evol.* **1993**, *10*, 60-72.

(18)Diaz, M.; Casali, P. Somatic immunoglobulin hypermutation. *Curr. Opi. Immun.* **2002**, *14*, 235-240.

(19)Wilson, J. J.; Burgess, R.; Mao, Y.-Q.; Luo, S.; Tang, H.; Jones, V. S.; Weisheng, B.; Huang, R.-Y.; Chen, X.; Huang, R.-P.: Chapter Seven - Antibody Arrays in Biomarker Discovery. In *Advances in Clinical Chemistry*; Gregory, S. M., Ed.; Elsevier, 2015; Vol. Volume 69; pp 255-324.

(20)Holford, T. R. J.; Davis, F.; Higson, S. P. J. Recent trends in antibody based sensors. *Biosens. Bioelectron.* **2012**, *34*, 12-24.

(21)Parker, D. C. T Cell-Dependent B Cell Activation. *Ann. Rev. Immun.* **1993**, *11*, 331-360.

(22)Justino, C. I. L.; Freitas, A. C.; Pereira, R.; Duarte, A. C.; Rocha Santos, T. A. P. Recent developments in recognition elements for chemical sensors and biosensors. *TrAC Trends in Anal. Chem.* **2015**, *68*, 2-17.

(23)Ruan, Q.; Tetin, S. Y. Applications of dual-color fluorescence cross-correlation spectroscopy in antibody binding studies. *Anal. Biochem.* **2008**, *374*, 182-195.

(24)Crisostomo, A. C.; Dang, L.; Digambaranath, J. L.; Klaver, A. C.; Loeffler, D. A.; Payne, J. J.; Smith, L. M.; Yokom, A. L.; Finke, J. M. Kinetic analysis of IgG antibodies to beta-amyloid oligomers with surface plasmon resonance. *Anal. Biochem*. **2015**, *481*, 43-54.

(25)Gao, J.; Guo, Z.; Su, F.; Gao, L.; Pang, X.; Cao, W.; Du, B.; Wei, Q. Ultrasensitive electrochemical immunoassay for CEA through host–guest interaction of β-cyclodextrin functionalized graphene and Cu@Ag core–shell nanoparticles with adamantine-modified antibody. *Biosens. Bioelectron.* **2015**, *63*, 465-471.

(26)Sargent, A.; Sadik, O. A. Monitoring antibody–antigen reactions at conducting polymer-based immunosensors using impedance spectroscopy. *Electrochim. Acta* **1999**, *44*, 4667-4675.

(27)Xiao, Y.; Li, C. M.; Liu, Y. Electrochemical impedance characterization of antibody–antigen interaction with signal amplification based on polypyrrole–streptavidin. *Biosens. Bioelectron.* **2007**, *22*, 3161-3166.

(28)Darain, F.; Park, S.-U.; Shim, Y.-B. Disposable amperometric immunosensor system for rabbit IgG using a conducting polymer modified screen-printed electrode. *Biosens. Bioelectron.* **2003**, *18*, 773-780.

(29)Huang, K.-J.; Niu, D.-J.; Xie, W.-Z.; Wang, W. A disposable electrochemical immunosensor for carcinoembryonic antigen based on nano-Au/multi-walled carbon nanotubes–chitosans nanocomposite film modified glassy carbon electrode. *Anal. Chim. Acta* **2010**, *659*, 102-108.

(30)Turner, A. P. F. Biosensors: sense and sensibility. *Chem. Soc. Rev.* **2013**, *42*, 3184-3196.

(31)Dong, S.; Wang, B. Electrochemical Biosensing in Extreme Environment. *Electroanal.* **2002**, *14*, 7-16.

(32)Ren, Z.; Gao, P.-X. A review of helical nanostructures: growth theories, synthesis strategies and properties. *Nanoscale* **2014**, *6*, 9366-9400.

(33)Zhu, C.; Yang, G.; Li, H.; Du, D.; Lin, Y. Electrochemical Sensors and Biosensors Based on Nanomaterials and Nanostructures. *Anal. Chem.* **2015**, *87*, 230-249.

(34)Li, N.; Su, X.; Lu, Y. Nanomaterial-based biosensors using dual transducing elements for solution phase detection. *Analyst* **2015**, *140*, 2916-2943.

(35)Pérez-López, B.; Merkoçi, A. Nanomaterials based biosensors for food analysis applications. *Tre. Food Sci. & Tech.* **2011**, *22*, 625-639.

(36)Chen, L.; Wu, B.; Guo, L.; Tey, R.; Huang, Y.; Kim, D.-H. A single-nanoparticle NO2 gas sensor constructed using active molecular plasmonics. *Chem. Commun.* **2015**, *51*, 1326-1329.

(37)Guo, L.; Huang, Y.; Kikutani, Y.; Tanaka, Y.; Kitamori, T.; Kim, D.-H. In situ assembly, regeneration and plasmonic immunosensing of a Au nanorod monolayer in a closed-surface flow channel. *Lab. Chip* **2011**, *11*, 3299-3304.

(38)Huang, Y.; Ferhan, A. R.; Gao, Y.; Dandapat, A.; Kim, D.-H. High-yield synthesis of triangular gold nanoplates with improved shape uniformity, tunable edge length and thickness. *Nanoscale* **2014**, *6*, 6496-6500.

(39)Huang, Y.; Ferhan, A. R.; Kim, D.-H. Tunable scattered colors over a wide spectrum from a single nanoparticle. *Nanoscale* **2013**, *5*, 7772-7775.

(40)Yu, Y.; Zhang, Q.; Lu, X.; Lee, J. Y. Seed-Mediated Synthesis of Monodisperse Concave Trisoctahedral Gold Nanocrystals with Controllable Sizes. *J. Phys. Chem. C* **2010**, *114*, 11119-11126.

(41)DeSantis, C. J.; Peverly, A. A.; Peters, D. G.; Skrabalak, S. E. Octopods versus Concave Nanocrystals: Control of Morphology by Manipulating the Kinetics of Seeded Growth via Co-Reduction. *Nano Lett.* **2011**, *11*, 2164-2168.

(42)Huang, Y.; Wu, L.; Chen, X.; Bai, P.; Kim, D.-H. Synthesis of Anisotropic Concave Gold Nanocuboids with Distinctive Plasmonic Properties. *Chem. Mater.* **2013**, *25*, 2470-2475.

(43)Lu, C.-L.; Prasad, K. S.; Wu, H.-L.; Ho, J.-a. A.; Huang, M. H. Au Nanocube-Directed Fabrication of Au–Pd Core–Shell Nanocrystals with Tetrahexahedral, Concave Octahedral, and Octahedral Structures and Their Electrocatalytic Activity. *J. Am. Chem. Soc.* **2010**, *132*, 14546-14553.

(44)Kannan, P.; Sampath, S.; John, S. A. Direct Growth of Gold Nanorods on Gold and Indium Tin Oxide Surfaces: Spectral, Electrochemical, and Electrocatalytic Studies. *The J. Phys. Chem. C* **2010**, *114*, 21114-21122.

(45)Kannan, P.; Tiong, H. Y.; Kim, D.-H. Highly sensitive electrochemical determination of neutrophil gelatinase-associated lipocalin for acute kidney injury. *Biosens. Bioelectron.* **2012**, *31*, 32-36.

(46)Kannan, P.; John, S. A. Highly sensitive determination of hydroxylamine using fused gold nanoparticles immobilized on sol–gel film modified gold electrode. *Anal. Chim. Acta* **2010**, *663*, 158-164.

(47)Kannan, P.; John, S. A. Highly sensitive electrochemical determination of nitric oxide using fused spherical gold nanoparticles modified ITO electrode. *Electrochim. Acta* **2010**, *55*, 3497-3503.

(48)Zhang, H.; Jin, M.; Xia, Y. Noble-Metal Nanocrystals with Concave Surfaces: Synthesis and Applications. *Angew. Chem. Inter. Ed.* **2012**, *51*, 7656-7673.

(49)Sohn, K.; Kim, F.; Pradel, K. C.; Wu, J.; Peng, Y.; Zhou, F.; Huang, J. Construction of Evolutionary Tree for Morphological Engineering of Nanoparticles. *ACS Nano* **2009**, *3*, 2191-2198.

(50)Huang, Y.; Kim, D.-H. Dark-field microscopy studies of polarization-dependent plasmonic resonance of single gold nanorods: rainbow nanoparticles. *Nanoscale* **2011**, *3*, 3228-3232.

(51)Keul, H. A.; Möller, M.; Bockstaller, M. R. Structural Evolution of Gold Nanorods during Controlled Secondary Growth. *Langmuir* **2007**, *23*, 10307-10315.

(52)Zhang, J.; Langille, M. R.; Personick, M. L.; Zhang, K.; Li, S.; Mirkin, C. A. Concave Cubic Gold Nanocrystals with High-Index Facets. *J. Am. Chem. Soc.* **2010**, *132*, 14012-14014.

(53)Tian, N.; Zhou, Z.-Y.; Sun, S.-G.; Ding, Y.; Wang, Z. L. Synthesis of Tetrahexahedral Platinum Nanocrystals with High-Index Facets and High Electro-Oxidation Activity. *Science* **2007**, *316*, 732-735.

(54)Alexeyeva, N.; Tammeveski, K. Electroreduction of oxygen on gold nanoparticle/PDDA-MWCNT nanocomposites in acid solution. *Anal. Chim. Acta* **2008**, *618*, 140-146.

(55)Kumar, S.; Zou, S. Electrooxidation of Carbon Monoxide on Gold Nanoparticle Ensemble Electrodes: Effects of Particle Coverage. *J. Phys. Chem. B* **2005**, *109*, 15707-15713.

(56)Kannan, P.; John, S. A. Ultrasensitive detection of l-cysteine using gold–5-amino-2-mercapto-1,3,4-thiadiazole core–shell nanoparticles film modified electrode. *Biosens. Bioelectron.* **2011**, *30*, 276-281.

(57)Lineweaver, H.; Burk, D. The Determination of Enzyme Dissociation Constants. *J. Am. Chem. Soc.* **1934**, *56*, 658-666.

Table of Content Entry
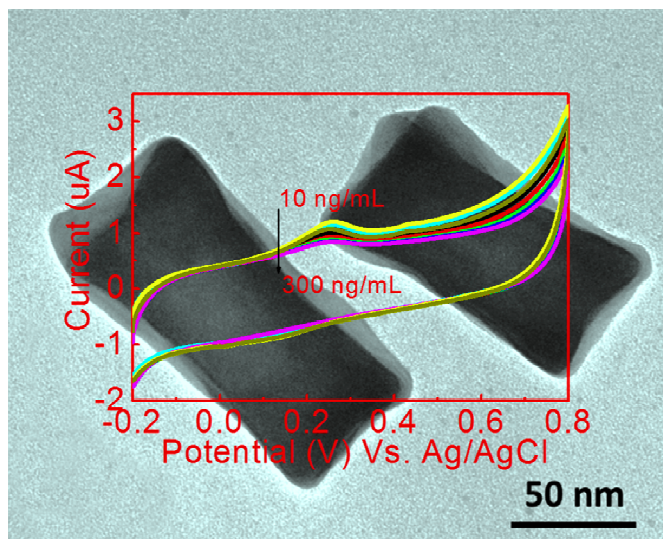
Concave gold nanocuboids based electrochemical sensor was developed for highly sensitive detection of antibody-antigen interactions.